DOI: 10.1103/PhysRevB.89.195308

Electron-electron interaction mediated indirect coupling of electron and magnetic ion or nuclear spins in self-assembled quantum dots

Udson C. Mendes,[1,2] Marek Korkusinski,[1] and Pawel Hawrylak[1,3,4]

[1]*Quantum Theory Group, Security and Disruptive Technologies, National Research Council, Ottawa, Canada K1A0R6*

[2]*Institute of Physics "Gleb Wataghin", State University of Campinas, Campinas, São Paulo, Brazil*

[3]*Department of Physics, University of Ottawa, Ottawa, Canada*

[4]*WPI-AIMR, Tohoku University, Sendai, Japan*

(Received 20 December 2013; revised manuscript received 12 April 2014; published 22 May 2014)

We show here the existence of the indirect coupling of electron and magnetic or nuclear ion spins in self-assembled quantum dots mediated by electron-electron interactions. With a single localized spin placed in the center of the dot, only the spins of electrons occupying the zero angular momentum states couple directly to the localized spin. We show that when the electron-electron interactions are included, the electrons occupying finite angular momentum orbitals interact with the localized spin. This effective interaction is obtained using exact diagonalization of the microscopic Hamiltonian as a function of the number of electronic shells, shell spacing, and anisotropy of the electron-Mn exchange interaction. The effective interaction can be engineered to be either ferromagnetic or antiferromagnetic by tuning the parameters of the quantum dot.

DOI: 10.1103/PhysRevB.89.195308 PACS number(s): 75.75.−c, 75.50.Pp, 78.67.Hc

I. INTRODUCTION

There is currently interest in understanding the coupling of a localized spin, either magnetic impurity or nuclear spin, with spins of interacting electrons [1,2]. This includes the Kondo effect in metals [3–7] and quantum dots [8–11], the impurity spin in diamond [12,13], charged quantum dots with magnetic ions [14–18], and nuclear spins coupled to fractional quantum Hall states [19–22]. Here we focus on a highly tunable system of quantum dots with a single magnetic ion and a controlled number of electrons. Such a system is realized in CdTe quantum dots with a magnetic impurity in the center of the dot loaded with a controlled, small at present, number of electrons [16]. The interplay between electron-electron Coulomb interactions and the electron-Mn exchange interaction has been studied using exact diagonalization techniques [15,17] and using the mean-field approach [14,23]. Other studies focused on electron-electron interactions in excitonic complexes coupled with localized spins [16,18,23–26].

Here we focus on the indirect coupling of electron and magnetic or nuclear ion spins in self-assembled quantum dots (QDs) mediated by the electron-electron interaction. With a localized spin placed in the center of the dot, only the spins of electrons occupying the zero angular momentum states of the $s,d,\ldots$ shells couple directly to the localized spin via a contact exchange interaction. The situation is identical to the Kondo problem in metals where only zero angular momentum states of the Fermi sea are considered as interacting with the localized spin. The question arises as to the role of electron-electron interactions. Here we show that, in quantum dots, when electron-electron interactions are included, the electrons occupying finite angular momentum orbitals (e.g., p shell) do interact with the localized spin. The effective interaction for p-shell electrons is obtained using exact diagonalization of the microscopic Hamiltonian as a function of the number of electronic shells, shell spacing, and anisotropy of the exchange interaction. The anisotropy of exchange interpolates between the interaction types characteristic for conduction band electrons (Heisenberg-like) and valence band holes (Ising-like). We show that the effective electron-electron mediated exchange interaction can be engineered to be either ferro- or antiferromagnetic by varying quantum-dot parameters.

The paper is organized as follows: In Sec. II we describe the model of a self-assembled quantum dot with a single Mn impurity in its center and a controlled number of electrons. Section III presents results of exact diagonalization of the model Hamiltonian for quantum dots confining from two to six electrons and the emergence of the indirect electron-Mn coupling for QDs with a partially filled p shell. Section IV summarizes our results.

II. MODEL

We consider a model system of N electrons ($N = 2,\ldots,6$) confined in a two-dimensional (2D) parabolic quantum dot with a single magnetic impurity in the center. Figure 1(a) illustrates a schematic representation of the investigated QD. For definiteness we consider an isoelectronic impurity, a manganese ion with a total spin $M = 5/2$ in a CdTe quantum dot [1]. In the effective mass and envelope function approximations, the single-particle states $|i,\sigma\rangle$ are those of a 2D harmonic oscillator (HO) with the characteristic frequency ω_0. They are labeled by two orbital quantum numbers, $i = \{n,m\}$, and the electron spin $\sigma = \pm 1/2$. The single-particle states are characterized by energy $E_{n,m} = \omega_0(n + m + 1)$ and angular momentum $L_e = n - m$. Figure 1(b) shows the single-particle states as a function of angular momentum. We express all energies in units of the effective Rydberg, $\mathrm{Ry}^* = m^* e^4/2\epsilon^2\hbar^2$, and all distances in units of the effective Bohr radius, $a_B^* = \epsilon\hbar^2/m^* e^4$, where m^*, e, ϵ, and $\hbar$ are respectively the electron effective mass and charge, the dielectric constant, and the reduced Planck constant. For CdTe we take $m^* = 0.1m_0$ and $\epsilon = 10.6$, where m_0 is the free-electron mass, and $\mathrm{Ry}^* = 12.11$ meV and $a_B^* = 5.61$ nm. Unless otherwise stated, we take the HO frequency $\omega_0 = 1.98\ \mathrm{Ry}^*$, consistent with our previous work [26].

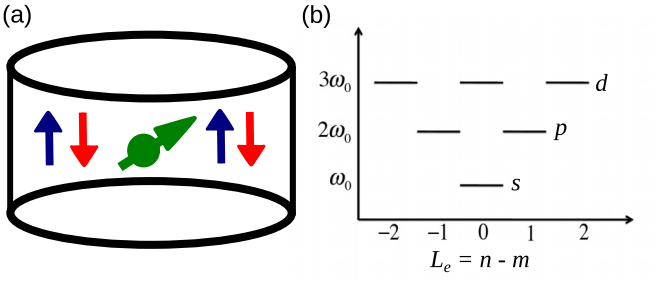

FIG. 1. (Color online) (a) Schematic representation of a CdTe quantum dot containing electrons and one Mn spin at its center. (b) Single-particle states as a function of angular momentum.

The Hamiltonian of N electrons confined in our QD and interacting with a single Mn spin is written as [15]

$$H = \sum_{i,\sigma} E_{i,\sigma} c^{\dagger}_{i,\sigma} c_{i,\sigma} + \frac{\gamma}{2} \sum_{\substack{i,j,k,l \\ \sigma,\sigma'}} \langle i,j|V_{ee}|k,l\rangle c^{\dagger}_{i,\sigma} c^{\dagger}_{j,\sigma'} c_{k,\sigma'} c_{l,\sigma} - \sum_{i,j} \frac{J_{i,j}(R)}{2} [(c^{\dagger}_{i,\uparrow} c_{j,\uparrow} - c^{\dagger}_{i,\downarrow} c_{j,\downarrow}) M_z + \varepsilon (c^{\dagger}_{i,\downarrow} c_{j,\uparrow} M^{+} + c^{\dagger}_{i,\uparrow} c_{j,\downarrow} M^{-})], \quad (1)$$

where $c^{\dagger}_{i,\sigma}$ ($c_{i,\sigma}$) creates (annihilates) an electron on the orbital $i = \{m,n\}$ with spin σ.

In the above Hamiltonian, the first term is the single-particle energy and the second term is the electron-electron (e-e) Coulomb interaction. The e-e term is scaled by a dimensionless parameter γ: $\gamma = 0$ describes the noninteracting electronic system and $\gamma = 1$ describes the interacting system. The matrix elements $\langle i,j|V_{ee}|k,l\rangle$ of the Coulomb interaction are evaluated in the basis of 2D HO orbitals in the closed form [27].

The last term of the Hamiltonian describes the electron-Mn interaction (e-Mn). It is scaled by the exchange coupling matrix elements $J_{i,j}(R) = J_C^{2D} \phi_i^*(R) \phi_j(R)$, where $J_C^{2D} = 2J_{\text{bulk}}/d$, $J_{\text{bulk}} = 15$ meV nm^3 is the s-d exchange constant for the CdTe bulk material, $d = 2$ nm is the QD height, and $\phi_i(R)$ is the amplitude of the HO wave function at the Mn position R. In particular, we define $J_{ss}(R) = J_C^{2D} \phi_s^*(R) \phi_s(R)$, which is the matrix element of an electron on the s shell interacting with a magnetic ion. For Mn at the QD center its value is $J_{ss} \approx 0.15$ meV.

The e-Mn interaction consists of two terms. The first one is the Ising interaction between the electron and Mn spin. The second term accounts for the e-Mn spin-flip interactions. The anisotropy of the exchange interaction is tuned by the factor ε. By setting $\varepsilon = 0$ we obtain the anisotropic Ising e-Mn exchange Hamiltonian and setting $\varepsilon = 1$ we obtain the isotropic Heisenberg exchange Hamiltonian. In the former case, the spin projections s_z and M_z are separately good quantum numbers. The total spin projection of the electrons depends on the number and polarization of the particles. For the manganese spin we have $M = 5/2$ and the six possible spin projections $M_z = -5/2, \ldots, 5/2$. The isotropic Heisenberg Hamiltonian, in contrast, conserves the total angular momentum $\mathbf{J} = \mathbf{M} + \mathbf{S}$ and its projection $J_z = s_z + M_z$. Hence, for the case $\varepsilon = 1$, one can establish the total spin quantum number J of the given manifold of states by considering its degeneracy $g(J) = 2J + 1$.

Since the elements $J_{i,j}$ depend on the position R of the Mn spin, the e-Mn coupling can be engineered by choosing a specific R [15]. In this work we place the Mn spin in the center of the QD and the only nonzero matrix elements $J_{i,j}$ appear if both orbitals i and j are zero angular momentum states. The spin of an electron placed on any other HO orbital is not coupled directly to the Mn spin.

The eigenenergies and eigenstates of the Hamiltonian (1) are obtained in the configuration-interaction approach. In this approach, we construct the Hamiltonian matrix in the basis of configurations of N electrons and one Mn spin: $|\nu_i\rangle = |i_{1\uparrow}, i_{2\uparrow}, \ldots, i_{N\uparrow}\rangle |j_{1\downarrow}, j_{2\downarrow}, \ldots, j_{N\downarrow}\rangle |M_z\rangle$, where $|i_{1\sigma}, i_{2\sigma}, \ldots, i_{N\sigma}\rangle = c^{\dagger}_{i_{1\sigma}} c^{\dagger}_{i_{2\sigma}}, \ldots, c^{\dagger}_{i_{N\sigma}} |0\rangle$, $|0\rangle$ is the vacuum state, and $N = N_{\uparrow} + N_{\downarrow}$ is the number of electrons, in which $N_{\uparrow}$ and $N_{\downarrow}$ are the number of electrons with spin up and spin down, respectively. The total number of configurations depends on the number of electrons and on the number of the HO shells available in the QD. With Mn impurity in the center, the total orbital angular momentum of electrons $L = \sum_{i=1}^{N} L_e^i$ is conserved by the Hamiltonian (1). Moreover, depending on the anisotropy of e-Mn interactions, the Hamiltonian also conserves the total projections S_z and M_z of the electron and Mn spin separately (the Ising model) or the projection $J_z = s_z + M_z$ of the total spin (the Heisenberg model). Based on these conservation rules, we divide the basis of configurations into subspaces labeled by the numbers L, S_z, and M_z (for the Ising model) or L and J_z (for the Heisenberg model), and diagonalize the Hamiltonian in each subspace separately.

Our model is also suitable for electrons interacting with a single nuclear spin. In the Fermi-contact hyperfine interaction [28], the Hamiltonian of electrons interacting with nuclear spins has the same form as the Hamiltonian of electrons interacting with Mn spins. Even though the interaction between electrons and single nuclear spins has not been achieved in self-assembled quantum dots, today it is possible to manipulate a few nuclear spins in diamond [29], silicon [30,31], and carbon nanotubes [32].

The computational procedure adopted in this work is as follows. For a chosen number of electrons $N = 2, \ldots, 6$ and a chosen number of HO shells, we look for the ground and several excited states for the system with and without e-e interactions in the Ising and isotropic Heisenberg models. By analyzing the degeneracies of the states we find the total spin of the system. Further, from the ordering of different states with respect to their total spin, we draw conclusions as to the ferromagnetic or antiferromagnetic character of the effective e-Mn interactions. By comparing the results for the system with and without the e-e interactions ($\gamma = 1$ or $\gamma = 0$, respectively) we establish the e-e interaction mediated effective e-Mn Hamiltonian for electrons not directly coupled to the central spin.

III. SPIN SINGLET CLOSED SHELLS COUPLED WITH THE MAGNETIC ION

We start with a discussion of a filled s shell with $N = 2$ electrons in the zero angular momentum channel. Each

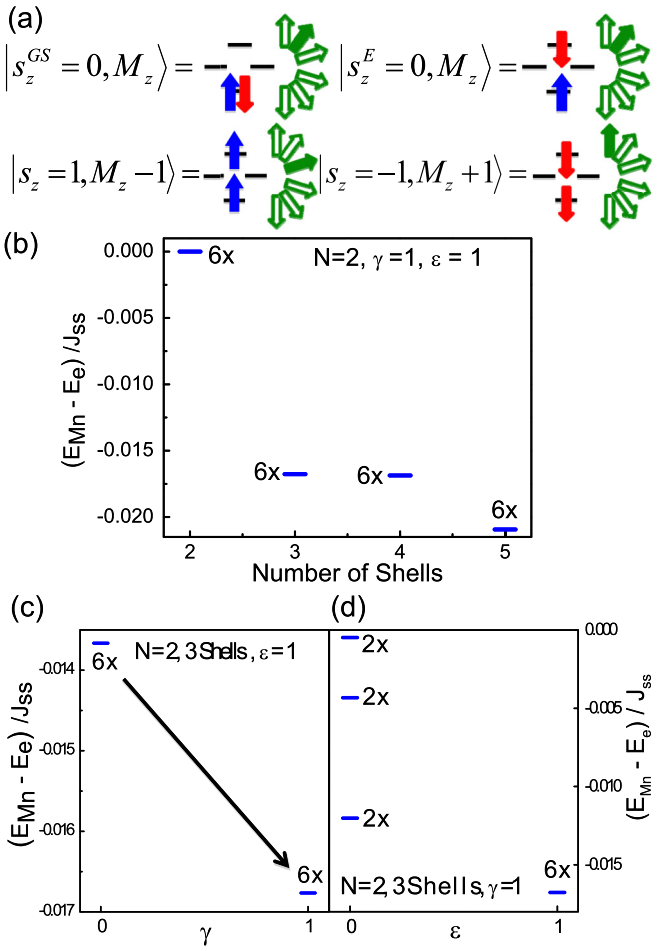

FIG. 2. (Color online) (a) Schematic pictures of two-electron-Mn configurations, GS and electronic triplet states, coupled by the e-Mn interactions. (b) Ground-state energy of the two-electron-Mn system as a function of the number of quantum-dot shells. (c) and (d) Ground-state energies of the two-electron-Mn system for the quantum dot confining three shells plotted as a function of the strength of electron-electron interactions in the Heisenberg e-Mn model (c) and as a function of the isotropy of the e-Mn Hamiltonian for the fully interacting electron system (d). Numbers at the energy level bars represent the degeneracy of states.

electron is directly coupled to the Mn impurity, but the singlet state couples only via e-e interactions [26]. Here we discuss the role of anisotropy of the exchange interaction on this indirect coupling. A similar discussion applies to other closed shells, e.g., $N=6$.

The lowest-energy s-shell spin singlet configuration with $S=0$ and orbital angular momentum $L=0$, $|s_z^{\rm GS}=0,M_z\rangle = c^\dagger_{s,\uparrow}c^\dagger_{s,\downarrow}|0,M_z\rangle$, is shown schematically in the top left panel of Fig. 2(a). The expectation value of the e-Mn Hamiltonian against the configuration $|s_z^{\rm GS}=0,M_z\rangle$ is zero.

Increasing the number of confined shells to three adds one additional orbital (1,1) with zero angular momentum in the d shell directly coupled to the Mn spin. Now the two-electron triplet states with total angular momentum $L=0$ couple to the Mn spin. The triplet with $S_z=0$, $|s_z^E=0,M_z\rangle = (1/\sqrt{2})(c^\dagger_{d,\uparrow}c^\dagger_{s,\downarrow}-c^\dagger_{s,\uparrow}c^\dagger_{d,\downarrow})|0\rangle|M_z\rangle$. One of its components is shown schematically in the top right panel of Fig. 2(a), while the bottom left panel of that figure shows the spin-polarized triplet $|s_z=1,M_z-1\rangle = c^\dagger_{s,\uparrow}c^\dagger_{d,\uparrow}|0,M_z-1\rangle$, and the bottom right panel shows the triplet $|s_z=-1,M_z+\rangle = c^\dagger_{s,\downarrow}c^\dagger_{d,\downarrow}|0,M_z+1\rangle$. Applying the e-Mn Hamiltonian to the $|s_z^{\rm GS}=0,M_z\rangle$ state, we obtain

$$H_{e\text{-Mn}}|s_z^{\rm GS}=0,M_z\rangle = -\frac{J_{sd}}{\sqrt{2}}M_z|s_z^E,M_z\rangle$$
$$-\frac{J_{sd}}{2}\varepsilon(\beta_-|s_z=1,M_z-1\rangle-\beta_+|s_z=-1,M_z+1\rangle), \quad (2)$$

where J_{sd} is the exchange matrix element in which one electron is scattered from the s orbital to the d orbital and $\beta_\pm = \sqrt{(M\mp M_z)(M\pm M_z+1)}$. We find that upon the inclusion of the d shell, the low-energy s-shell singlet two-electron configuration becomes coupled by e-Mn interactions to electron triplet configurations, with and without flip of the Mn spin.

We now diagonalize the two-electron-Mn Hamiltonian and compute the ground-state (GS) energy $E_{\rm Mn}$ of the QD with a manganese ion, and the energy E_e of the system without Mn. Figure 2(b) shows the effect of the Mn ion on the ground-state energy, $\Delta=(E_{\rm Mn}-E_e)/J_{ss}$, measured from the ground-state energy without the Mn ion, as a function of the number of shells for the interacting system ($\gamma=1$) and the isotropic exchange interaction ($\varepsilon=1$). We find that, irrespective of the number of confined shells, the GS is sixfold degenerate, with the total spin $J_{\rm GS}=5/2$. However, the energy of the GS markedly depends on the number of shells. For two confined shells we have $\Delta=0$, because in this case we can generate only one configuration, $|s_z^{\rm GS}=0,M_z\rangle$, which is decoupled from the Mn spin. The inclusion of the d shell adds an additional $L_e=0$ orbital into the single-particle basis, resulting in the scattering of electrons by the localized spin and lowering of energy. A further lowering of the energy occurs when the fifth shell, containing another $L_e=0$ single-particle state, becomes confined.

Now we fix the number of shells to three, set the Heisenberg form of e-Mn interactions, and study the effect of e-e interactions. Figure 2(c) shows the energy Δ without ($\gamma=0$) and with full Coulomb interactions ($\gamma=1$). We find that the ground state in both cases is sixfold degenerate but the e-e Coulomb interactions enhance the effects of the e-Mn coupling, lowering Δ. This is due to a larger contribution of triplet configurations to the GS.

We now compare the results for the isotropic coupling versus the anisotropic coupling. For the anisotropic coupling, $\varepsilon=0$, we observe that the GS is split into three energy levels labeled by $|M_z|$, each of them twice degenerate, as shown in Fig. 2(d). In Ising-like coupling the total angular momentum J is not conserved, and the characteristic sixfold degeneracy of the ground state is broken. Comparing the isotropic and anisotropic coupling, we observe that Δ is negative for both couplings and also that the Heisenberg-like interaction results in a lower energy than the Ising-like interaction [26].

IV. ELECTRONS IN FINITE ANGULAR MOMENTUM CHANNELS

In this section we discuss electrons populating finite angular momentum channels which are not directly coupled with the

Mn ion. For $N = 3$ we show the existence of an effective coupling mediated by e-e interactions. Similar results are obtained for $N = 5$.

A. One electron on the p shell

The lowest-energy configuration in the ground state of three electrons is formed by two electrons in the s shell and one electron in the p shell. With Mn in the QD center the total angular momentum L of the three electrons is conserved and we show the results for $L = 1$.

Figure 3(a) illustrates the degenerate three-electron configurations, $|s_z = 1/2, M_z\rangle$ and $|s_z = -1/2, M_z + 1\rangle$, with an electron with spin up and Mn in state M_z and an electron with spin down on the p orbital and Mn in state $M_z + 1$. As the electron-Mn exchange interaction in the p shell vanishes, $J_{pp} = 0$, these configurations do not interact with each other.

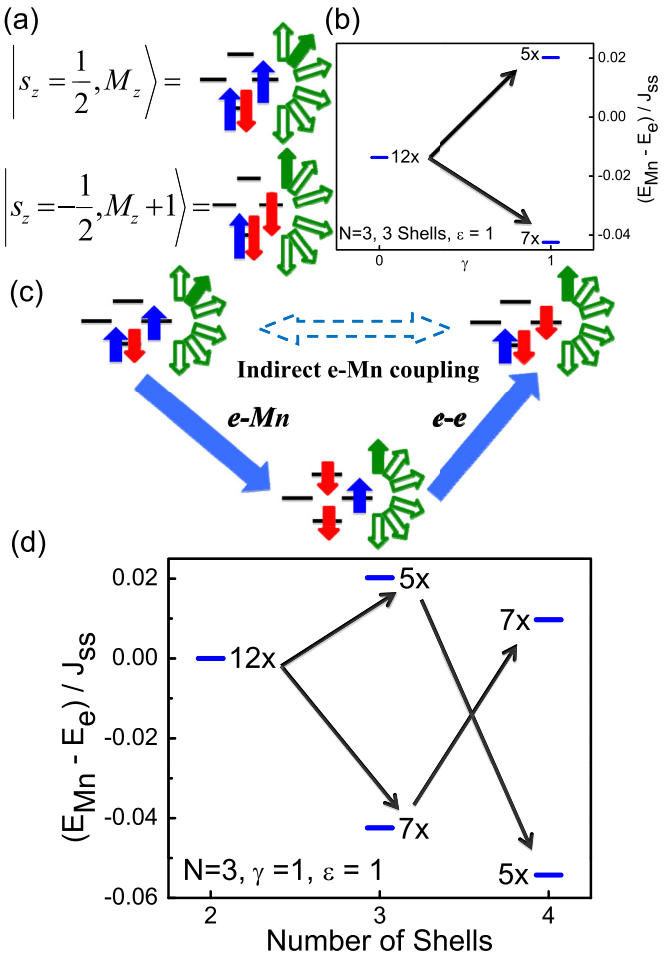

FIG. 3. (Color online) (a) Ground-state three-electron configurations with the p-shell electron spin up (top) and spin down (bottom). (b) Energy difference Δ between a three-electron GS in the Mn-doped and undoped QD for both noninteracting ($\gamma = 0$) and interacting ($\gamma = 1$) electrons. The numbers indicate the degeneracy of each level. (c) Diagram of coupling between electrons in the p shell and Mn. The solid arrow represents a direct coupling via e-Mn coupling or e-e Coulomb interaction, and the dashed arrow illustrates the indirect coupling. (d) The energy difference Δ as a function of the number of shells for a QD containing three shells and $\gamma = 1$.

As a consequence, the GS is 12-fold degenerate, two electron spin configurations times six Mn spin orientations. In order to understand the effect of interactions we include configurations coupled with $|s_z = 1/2, M_z\rangle$ and $|s_z = -1/2, M_z + 1\rangle$ by both e-e and e-Mn interactions and diagonalize the Hamiltonian in the $L = 1$ subspace. The number of three-electron-Mn configurations depends on the number of electronic shells, with 24, 228, 852, and 2520 for two, three, four, and five shells, respectively.

Figure 3(b) shows the result of exact diagonalization of the e-Mn Hamiltonian for three confined shells in the QD and an isotropic e-Mn interaction ($\epsilon = 1$), for both noninteracting ($\gamma = 0$) and interacting ($\gamma = 1$) electron systems. For the noninteracting case we observe that the GS is 12-fold degenerate, with the energy lowered by the e-Mn interaction (negative Δ). This behavior is identical to what was shown for the two electrons in the previous section, i.e., the two electrons in the s shell are coupled with Mn, while the electron in the p shell is only a spectator. However, in the strongly interacting regime, $\gamma = 1$, we observe a splitting of the degenerate GS into two degenerate shells. The splitting and the degeneracy of levels is consistent with an effective Hamiltonian $H_{\text{eff}} = -J_{\text{eff}}\vec{s}\cdot\vec{M}$ coupling the p-shell electron spin s with Mn spin M [15]. The effective coupling J_{eff} is mediated by Coulomb interactions. In Fig. 3(c) we illustrate the processes which couple $|s_z = 1/2, M_z\rangle$ and $|s_z = -1/2, M_z + 1\rangle$ states. The e-Mn interaction acting on the $|s_z = 1/2, M_z\rangle$ state scatters the spin-up (blue) electron from the s shell to the spin-down (red) electron on the d shell with a simultaneous transition of the Mn spin from M_z to $M_z + 1$. In the next step, the e-e interaction scatters the d-shell and p-shell electron pair into the s-shell and p-shell electron pair, with the spin-down electron on the p shell and the spin-up electron on the s shell. The net result is a spin flip of the p-shell electron and of the Mn spin. We see that the ground state is sevenfold degenerate, implying that the electron spin is aligned with the Mn spin and J_{eff} is hence ferromagnetic.

Let us now investigate the dependence of the GS energy on the number of confined shells in the QD. Figure 3(d) shows the evolution of the GS energy as a function of the number of shells for $\gamma = 1$ and $\varepsilon = 1$. We observe that for two shells there is no splitting, i.e., $J_{\text{eff}} = 0$, while for three and four shells the GS is split into two shells. For two shells the GS is 12-fold degenerate, $\Delta = 0$, and there is no interaction between Mn and electrons. For three shells the GS is split into two shells, as discussed above. For four shells the GS is also split into two, but there is an inversion of the degeneracy of the energy levels. This is a consequence of an antiferromangetic interaction $J_{\text{eff}} < 0$ between the electron and Mn spins. We also have observed that for QDs confining five or six shells the results are similar to what was obtained for QD with four shells, i.e., the antiferromagetic coupling is stabilized for a QD containing more than three confined shells. This can be understood by looking at the way the GS is coupled to Mn. In Fig. 3(c) we show that there is an indirect coupling between configurations $|s_z = 1/2, M_z\rangle$ and $|s_z = -1/2, M_z + 1\rangle$ which is mediated via e-e Coulomb and e-Mn interactions between the GS and excited configurations. As the number of shells increases, more excited state configurations interact with the GS, stabilizing the antiferromagnetic indirect coupling between the electrons and Mn.

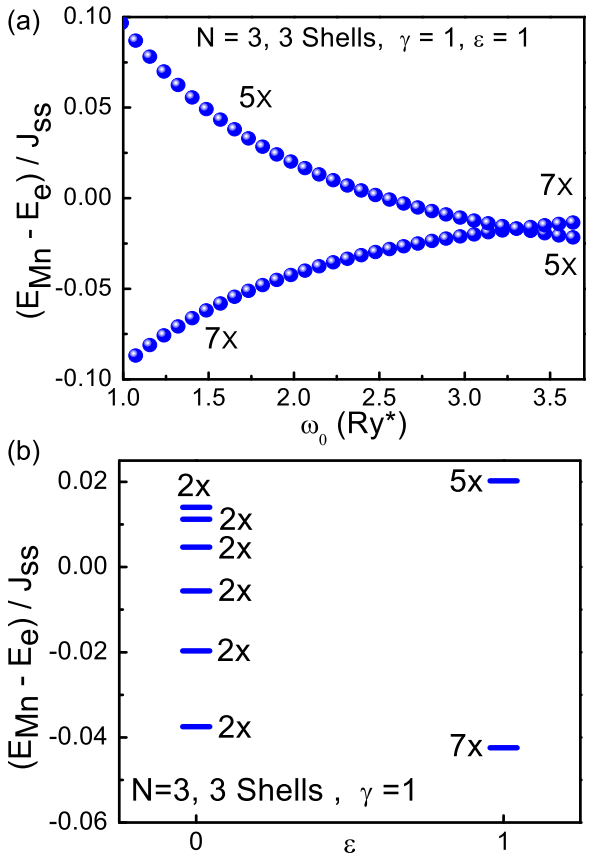

FIG. 4. (Color online) (a) Evolution of the energies of three-electron levels with $J = 3$ and $J = 2$ as a function of the QD shell spacing ω_0. (b) Energy difference Δ for both anisotropic ($\varepsilon = 0$) and isotropic ($\varepsilon = 1$) e-Mn interactions in a three-shell QD with full interactions ($\gamma = 1$).

If the indirect magnetic ordering shown above depends on the number of shells, it also should depend on the QD shell spacing ω_0. Figure 4(a) shows the dependence of GS energy on ω_0 for three electrons confined in a Mn-doped QD containing three shells, $\gamma = 1$ and $\varepsilon = 1$. We note that the exchange coupling changes from ferromagnetic to antiferromagnetic for $\omega_0 \approx 3.3$ Ry*. We observe the same behavior for QDs with four shells, but in this case the crossing occurs at $\omega_0 \approx 0.45$ Ry*.

Next we discuss the effect of anisotropy on the e-Mn exchange interaction. Figure 4(b) shows the GS energy for three electrons in a QD containing three shells in the strongly interacting regime as a function of the e-Mn coupling. For $\epsilon = 0$ the electrons and Mn interact via an anisotropic Ising-like Hamiltonian, and for $\epsilon = 1$ the e-Mn interaction is isotropic, Heisenberg-like. For $\epsilon = 0$, s_z is a good quantum number, and therefore the electron spin degeneracy is preserved. In Fig. 4(b) we observe that for $\epsilon = 0$ the energy spectrum is split into six doubly degenerate levels. This splitting is due to the e-e Coulomb interaction driving the indirect e-Mn interaction between the p-shell electron and Mn, as was observed in the $\epsilon = 1$ case. The double degeneracy for the anisotropic coupling arises due to the fact that the state $|s_z = 1/2, M_z\rangle$ has the same energy as the configuration of $|s_z = -1/2, -M_z\rangle$.

We also investigated the effect of Mn positions on three-electron GSs. Moving Mn away from the QD center couples the electron in the p orbital directly with Mn. This coupling is ferromagnetic. Considering a QD containing three shells and $\omega = 1.98$ Ry*, the indirect e-Mn coupling is also ferromagnetic, and therefore both direct and indirect e-Mn interactions add up. As Mn is moved away from the QD center, the direct coupling becomes the dominant effect for Mn positions larger than $R \approx 0.2 l_0$. Even though the direct e-Mn interaction is dominant for Mn far away of the QD center, the indirect e-Mn coupling is always present.

B. Two spin-polarized electrons on the p shell

Next we describe the electronic properties of a half-filled p shell. The lowest-energy configuration of the four-electron GS state is formed by two electrons in the s shell and two spin triplet electrons in the p shell. Figure 5(a) illustrates the four-electron configurations, the triplet $|S = 1, s_z = 1, M_z\rangle$ and one of the singlet component $|S = 0, s_z = 0, M_z + 1\rangle$ configurations. These two configurations have the same total spin projection J_z. In the presence of an e-e Coulomb interaction the $S = 1$ triplet state is the GS and the singlet is an excited state. For Mn in the QD center the p electrons do not couple with Mn, the electron spin degeneracy is preserved, and the degeneracy of the triplet state in a Mn-doped QD is 18, while the singlet state is sixfold degenerate.

We shall now investigate how the GS of four electrons confined in a Mn-doped QD is affected by the presence of the e-e Coulomb interaction, number of shells, shell spacing, and e-Mn coupling. We take advantage of the conservation of the total angular momentum and diagonalize our microscopic Hamiltonian in the $L = 0$ subspace. The number of configurations in this subspace is 30, 498, and 3498 for two, three, and four shells, respectively.

The e-e mediated coupling of the electronic and Mn spin is interpreted in terms of the effective exchange Hamiltonian. Adding the electron and Mn spins results in total spin $J = 7/2, 5/2, 3/2$ and splitting of the 18-fold degenerate ground state into eightfold, sixfold, and fourfold degenerate shells. Figure 5(b) shows the evolution of the low-energy part of the spectrum of four electrons in the magnetic dot as a function of the number of shells for full e-e interactions ($\gamma = 1$) and the isotropic e-Mn coupling ($\varepsilon = 1$). The energies of these states are shown relative to the energy of the ground-state triplet of the undoped QD. The triplet and singlet states split for any number of shells due to an e-e exchange interaction. In a QD with only s and p shells, the effective exchange coupling for p-shell electrons is zero and the triplet and singlet states are 18 and six times degenerate, respectively. Increasing the number of shells leads to a finite and ferromagnetic exchange interaction with the triplet states coupled to the Mn spin and the 18-fold degenerate shell split into eight-, six- and fourfold degenerate levels. The character of this exchange interaction depends on the number of shells. For three shells we have a ferromagnetic coupling, but for four shells the coupling becomes antiferromagnetic.

Figure 5(c) illustrates the configurations involved in the indirect coupling of the electrons on the p shell and the Mn spin. Here, the solid arrows represent the direct coupling

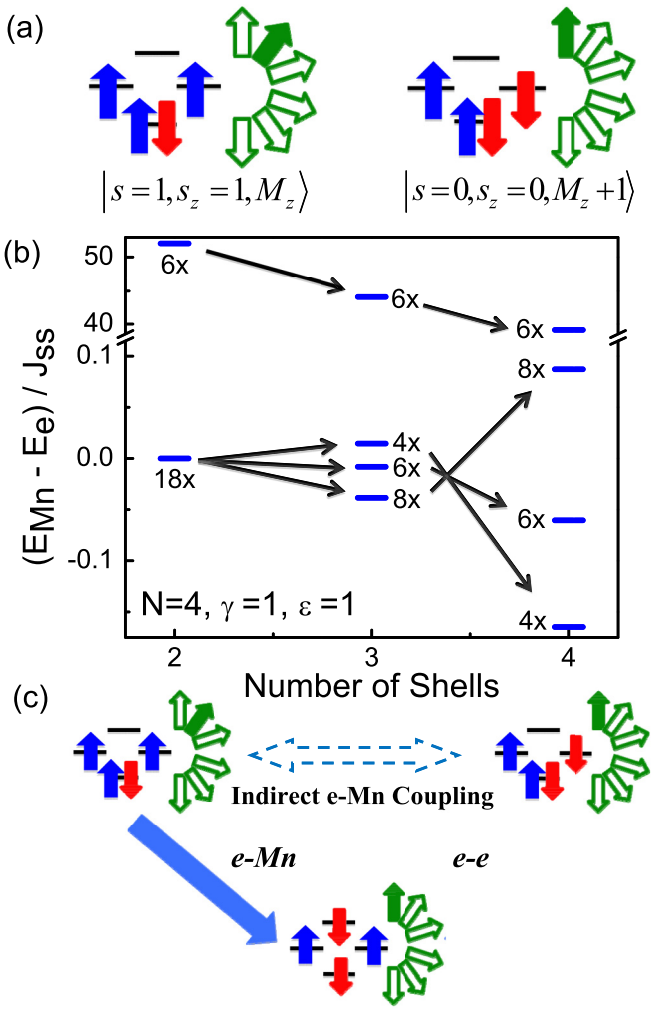

FIG. 5. (Color online) (a) Low-energy configurations of four electrons in a magnetic QD. (b) Low-energy spectrum of the system as a function of the number of shells for interacting ($\gamma = 1$) electrons, measured from the respective GS energy E_e of a nonmagnetic system. Here the QD shell spacing $\omega_0 = 1.98$ Ry*. (c) Indirect coupling diagram of two four-electron configurations. The solid arrows represent direct interactions between configurations and the dashed arrow represents the indirect e-Mn coupling.

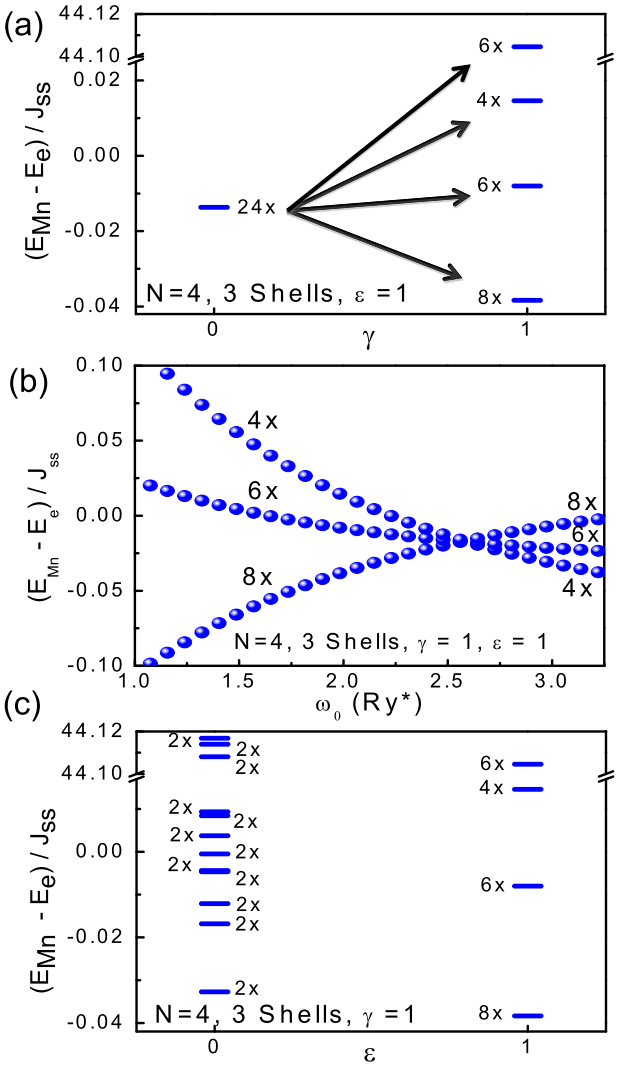

FIG. 6. (Color online) (a) Energy difference Δ for noninteracting ($\gamma = 0$) and interacting ($\gamma = 1$) electrons in the four-electron magnetic dot. (b) GS energy difference as a function of the QD shell spacing ω_0 for three shells confined in the QD. (c) GS energy difference for the anisotropic ($\varepsilon = 0$) and isotropic ($\varepsilon = 1$) e-Mn coupling.

between configurations, and the dashed arrow represents the indirect interaction between two configurations. Let us explain how this indirect coupling arises, starting from the configuration with two spin-up electrons in the p shell, which is labeled as $|S = 1, s_z = 1, M_z\rangle$ [see Fig. 5(c), top left]. This configuration is coupled with an excited state in which there are two spin-down electrons in both $L_e = 0$ orbitals, one in the s shell and the other in the d shell. This coupling occurs via an e-Mn interaction, which scatters the spin-up electron in the s shell of $|S = 1, s_z = 1, M_z\rangle$ to the d shell, flipping the electron spin down, and the Mn spin up, i.e., $M_z + 1$. This excited state with $s_z = 0$ and $M_z + 1$ is coupled with one of the $|S = 0, s_z = 0, M_z + 1\rangle$ GS configurations via the e-e Coulomb interaction, in which the spin-down electron in the d shell is scattered to the $L_e = 1$ p orbital, and the spin-up electrons in this orbital are scattered to the s shell.

Figure 6(a) shows the GS energy for both noninteracting ($\gamma = 0$) and fully interacting ($\gamma = 1$) electrons. We considered a Mn-doped QD with three confined shells and the isotropic e-Mn interaction ($\varepsilon = 1$). For the noninteracting case there is no triplet-singlet splitting, and as an e-e Coulomb interaction mediates the indirect interaction between Mn and the p-shell electrons, the triplet is not split either. Therefore, the four-electron GS is 24-fold degenerate. Even though the four noninteracting electron triplet states are not split by the indirect coupling, we see a negative Δ, which means that electrons lower their energy by an exchange interaction with Mn. Turning the e-e Coulomb interaction on results in the singlet-triplet splitting and a further splitting of the triplet energy shell. The triplet splitting is caused by the indirect interaction between Mn and electrons in the p shell, which is mediated by the e-e Coulomb interaction.

In Fig. 6(a) we show the effect of the *e*-*e* Coulomb interaction on the low-energy spectrum of the four-electron and Mn complex. We note the appearance of triplet and singlet energy shells, separated by the *e*-*e* exchange interaction. The splitting of the triplet shell is governed by the *e*-*e* and *e*-Mn exchange interactions.

Figure 6(b) presents the energy difference Δ, i.e., the effective exchange coupling, as a function of ω_0 for four interacting electrons ($\gamma = 1$) confined in the Mn-doped QD with three confined shells. Here we also have a ferromagnetic to antiferromagnetic crossing as a function of the QD shell spacing. For QDs with four shells the ferromagnetic to antiferromagnetic crossing occurs at $\omega_0 \approx 0.04$ Ry*.

Now we show the effect of the symmetry of the *e*-Mn coupling on the four-electron GS. In Fig. 6(c) we compare the effects of the anisotropic ($\varepsilon = 0$) and isotropic ($\varepsilon = 1$) coupling for a Mn-doped QD with three confined shells and in the presence of a full *e*-*e* Coulomb interaction ($\gamma = 1$). For the anisotropic coupling the triplet state is split into nine doubly degenerate levels. In this case, both s_z and M_z are good quantum numbers, and therefore $s_z = 1$ and $s_z = -1$ breaks the Mn spin degeneracy into six. As the energy of the state with $s_z = 1$ and M_z is equal to the energy of the state $s_z = -1$ and $-M_z$, these six states are double degenerate. The $s_z = 0$ configurations split into three, where the degeneracy is given by M_z, i.e., the $s_z = 0$ configurations are degenerate and labeled by $|M_z|$, as for the two electrons interacting with the Mn via an anisotropic *e*-Mn interaction. The singlet state is also split into three doubly degenerate levels.

One way to probe the indirect *e*-Mn interaction is by performing a circularly polarized photoluminescence experiment of quantum dots containing a single Mn spin and confining three or more electrons. In this case, the indirect *e*-Mn coupling gives rise to a fine structure of both initial and final states of the emission process [18].

V. CONCLUSION

In conclusion, we presented a microscopic model of interacting electrons coupled with a magnetic ion spin localized in the center of a self-assembled quantum dot. We showed that the electrons occupying finite angular momentum orbitals interact with the localized spin through an effective exchange interaction mediated by electron-electron interactions. The effective interaction for *p*-shell electrons is obtained using exact diagonalization of the microscopic Hamiltonian as a function of the number of electronic shells, shell spacing, and anisotropy of the exchange interaction. It is shown that the effective interaction can be engineered to be either ferro- or antiferromagnetic, depending on the quantum-dot parameters.

ACKNOWLEDGMENTS

The authors thank NSERC and the Canadian Institute for Advanced Research for support. U.C.M. thanks J. A. Brum for fruitful discussions and acknowledges the support from CAPES-Brazil (Project No. 5860/11-3) and FAPESP-Brazil (Project No. 2010/11393-5). P.H. thanks Y. Hirayama, WPI-AIMR, Tohoku University for hospitality.

[1] P. Hawrylak, in *The Physics of Diluted Magnetic Semiconductors*, edited by J. Gaj and J. Kossut, Springer Series in Materials Science (Springer, Berlin, 2011).
[2] P. M. Koenraad and M. E. Flatté, Nat. Mater. **10**, 91 (2011).
[3] J. Kondo, Prog. Theor. Phys. **32**, 37 (1964).
[4] A. C. Hewson, *The Kondo Problem to Heavy Fermions* (Cambridge University Press, Cambridge, UK, 1993).
[5] V. Madhavan, W. Chen, T. Jamneala, M. F. Crommie, and N. S. Wingreen, Science **280**, 567 (1998).
[6] J. Li, W.-D. Schneider, R. Berndt, and B. Delley, Phys. Rev. Lett. **80**, 2893 (1998).
[7] D. Jacob, M. Soriano, and J. J. Palacios, Phys. Rev. B **88**, 134417 (2013).
[8] D. Goldhaber-Gordon, H. Shtrikman, D. Mahalu, D. Abusch-Magder, U. Meirav, and M. A. Kastner, Nature (London) **391**, 156 (1998).
[9] S. M. Cronenwett, T. H. Oosterkamp, and L. P. Kouwenhoven, Science **281**, 540 (1998).
[10] N. A. J. M. Kleemans, J. van Bree, A. O. Govorov, J. G. Keizer, G. J. Hamhuis, R. Nötzel, A. Yu. Silov, and P. M. Koenraad, Nat. Phys. **6**, 534 (2010).
[11] C. Latta, F. Haupt, M. Hanl, A. Weichselbaum, M. Claassen, W. Wuester, P. Fallahi, S. Faelt, L. Glazman, J. von Delft, H. E. Türeci, and A. Imamoglu, Nature (London) **474**, 627 (2011).
[12] G. Balasubramanian, I. Y. Chan R. Kolesov, M. Al-Hmoud, J. Tisler, C. Shin, C. Kim, A. Wojcik, P. R. Hemmer, A. Krueger, T. Hanke, A. Leitenstorfer, R. Bratschitsch, F. Jelezko, and J. Wrachtrup, Nature (London) **455**, 648 (2008).
[13] H. J. Mamin, M. Kim, M. H. Sherwood, C. T. Rettner, K. Ohno, D. D. Awschalom, and D. Rugar, Science **339**, 557 (2013).
[14] A. O. Govorov, Phys. Rev. B **70**, 035321 (2004).
[15] F. Qu and P. Hawrylak, Phys. Rev. Lett. **95**, 217206 (2005).
[16] Y. Leger, L. Besombes, J. Fernandez-Rossier, L. Maingault, and H. Mariette, Phys. Rev. Lett. **97**, 107401 (2006).
[17] N. T. T. Nguyen and F. M. Peeters, Phys. Rev. B **78**, 245311 (2008).
[18] U. C. Mendes, M. Korkusinski, A. H. Trojnar, and P. Hawrylak, Phys. Rev. B **88**, 115306 (2013).
[19] T. Machida, S. Ishizuka, T. Yamazaki, S. Komiyama, K. Muraki, and Y. Hirayama, Phys. Rev. B **65**, 233304 (2002).
[20] G. Yusa, K. Muraki, K. Takashina, K. Hashimoto, and Y. Hirayama, Nature (London) **434**, 1001 (2005).
[21] M. H. Fauzi, S. Watanabe, and Y. Hirayama, Appl. Phys. Lett. **101**, 162105 (2012).
[22] K. Akiba, T. Yuge, S. Kanasugi, K. Nagase, and Y. Hirayama, Phys. Rev. B **87**, 235309 (2013).
[23] A. O. Govorov and A. V. Kalameitsev, Phys. Rev. B **71**, 035338 (2005).
[24] J. Fernandez-Rossier, Phys. Rev. B **73**, 045301 (2006).
[25] A. H. Trojnar, M. Korkusinski, E. S. Kadantsev, P. Hawrylak, M. Goryca, T. Kazimierczuk, P. Kossacki, P. Wojnar, and M. Potemski, Phys. Rev. Lett. **107**, 207403 (2011).

[26] A. H. Trojnar, M. Korkusinski, U. C. Mendes, M. Goryca, M. Koperski, T. Smolenski, P. Kossacki, P. Wojnar, and P. Hawrylak, Phys. Rev. B **87**, 205311 (2013).
[27] P. Hawrylak, Solid State Commun. **88**, 475 (1993).
[28] B. Urbaszek, X. Marie, T. Amand, O. Krebs, P. Voisin, P. Maletinsky, A. Högele, and A. Imamoglu, Rev. Mod. Phys. **85**, 79 (2013).
[29] S.-Y. Lee, M. Widmann, T. Rendler, M. W. Doherty, T. M. Babinec, S. Yang, M. Eyer, P. Siyushev, B. J. M. Hausmann, M. Loncar, Z. Bodrog, A. Gali, N. B. Manson, H. Fedder, and J. Wrachtrup, Nat. Nanotechnol. **8**, 487 (2013).
[30] A. Morello, J. J. Pla, F. A. Zwanenburg, K. W. Chan, K. Y. Tan, H. Huebl, M. Möttönen, C. D. Nugroho, C. Yang, J. A. van Donkelaar, A. D. C. Alves, D. N. Jamieson, C. C. Escott, L. C. L. Hollenberg, R. G. Clark, and A. S. Dzurak, Nature (London) **467**, 687 (2010).
[31] K. Saeedi, S. Simmons, J. Z. Salvail, P. Dluhy, H. Riemann, N. V. Abrosimov, P. Becker, H.-J. Pohl, J. J. L. Morton, and M. L. W. Thewalt, Science **342**, 830 (2013).
[32] H. O. H. Churchill, A. J. Bestwick, J. W. Harlow, F. Kuemmeth, D. Marcos, C. H. Stwertka, S. K. Watson, and C. M. Marcus, Nat. Phys. **5**, 321 (2009).